



In vitro and *in vivo* biofilm inhibitory efficacy of geraniol-cefotaxime combination against *Staphylococcus* spp.

Arunachalam Kannappan, Boopathi Balasubramaniam, Rajendhran Ranjitha, Ramanathan Srinivasan, Issac Abraham Sybiya Vasantha Packiavathy, Krishnaswamy Balamurugan, Shunmugiah Karutha Pandian, Arumugam Veera Ravi*

Department of Biotechnology, Alagappa University, Science Campus, Karaikudi, 630 003, Tamil Nadu, India

ARTICLE INFO

Keywords:
Antibiofilm
Caenorhabditis elegans
Cefotaxime
Geraniol
Staphylococcus spp

ABSTRACT

In humans, the occurrence of bacterial communities in the form of biofilm is considered as a major intrinsic factor accountable for a variety of stubborn infections. *Staphylococcus aureus* and *S. epidermidis* have gained considerable attention in clinical settings owing to the formation of intractable and long-lasting biofilms in medical device. The current study has been designed to explain the biofilm inhibitory efficacy of geraniol and cefotaxime combination (GCC) against *S. epidermidis* and methicillin-resistant *S. aureus* (MRSA). Biofilm biomass quantification assay was performed to evaluate the antibiofilm activity of GCC against *S. epidermidis* and MRSA. The minimal biofilm inhibitory concentration of GCC was found to be 100 µg/ml of geraniol and 2 µg/ml of cefotaxime. Further, microscopic analyses ascertained the devastating potential of GCC on the test pathogens' biofilm formation. Besides biofilm inhibition, GCC also suppressed the production of extracellular polymeric substance, slime and staphyloxanthin. More, GCC significantly increased the susceptibility of the test pathogens towards human blood. Further, the results of real time PCR analysis and *in vivo* assay using *Caenorhabditis elegans* unveiled the anti-biofilm potentials of GCC. Thus, the present study demonstrates the significant use of polytherapy treatment approaches to overcome the biofilm associated infections of *Staphylococcus* spp.

1. Introduction

Microbial biofilm formation in nature is considered to be a sophisticated, dynamic and multifaceted development process (Kostakioti et al., 2013). The shift of planktonic growth to biofilm mode of growth enables the bacterial cells to survive in harsh environmental conditions by altering the cellular programs such as expression of surface molecules, virulence factors production and utilization of nutrients (Flemming et al., 2016). Within the biofilm, bacterial cells wrap themselves in a self-secreted extracellular polymeric substance (EPS), which accounts for 90% of the biofilm biomass. EPS consist of secreted enzymes, proteins, eDNA and polysaccharides. It acts as a scaffold for maintaining biofilm architecture and gives high tensile strength to keep the bacterial cells in close vicinity. It also protects the biofilm inhabitants from desiccation, predation, oxidizing molecules, radiation and other damaging agents (Kostakioti et al., 2013).

In human, the occurrence of bacterial communities in the form of biofilm is considered as a major intrinsic factor accountable for a variety of stubborn infections like central venous catheter infection,

endocarditis, etc. (Lebeaux et al., 2014). The correlation between bacterial biofilms and medical implants has been well documented in many pathogenic bacteria and their deleterious effects are of great concern in the medical community (Davies, 2003). Prophylactic treatment methods using antibiotics have proven its potential against bacterial infections over several years. However, the rise of multidrug resistant, pandrug resistant and extremely drug resistant organisms, the antibiotic treatment has very little or no preventive effect on infections caused by such organisms (Lebeaux et al., 2014). Therefore, the search of much more effective treatment method that target biofilm formation and virulence factors production became imperative.

Plants and plant-derived phytochemicals are one among the alternatives being explored presently. Because of their structural diversity, phytochemicals act as a base for the structural manipulations to obtain synthetic compounds with enhanced activity (Phillipson, 2001). Compared to monotherapy, combination therapy (polytherapy) is a new treatment strategy and now has been proven for its inhibitory potential against multidrug resistant bacterial infections especially against Gram-positive bacteria (Simoes, 2011). Combination therapy

* Corresponding author.

E-mail address: aveeraravi@rediffmail.com (A.V. Ravi).

<https://doi.org/10.1016/j.fct.2019.01.008>

Received 24 October 2018; Received in revised form 9 January 2019; Accepted 10 January 2019

Available online 14 January 2019

0278-6915/ © 2019 Elsevier Ltd. All rights reserved.

has numerous benefits over monotherapy, including the treatment for mixed infections, increased bioactivity even at low concentrations, multi-targeted mode of actions, preventing the emergence of multidrug resistance, etc (Bulusu et al., 2016). Geraniol (GE), an acyclic monoterpene alcohol, is naturally occurring as major constituent in the essential oils of lime, lemongrass, lavender and has been studied for its wide range of biological activities such as antimicrobial, anti-inflammatory, antitumor, etc. (Jeong et al., 2012). Cefotaxime (3-acetoxymethyl-7-[(2-(2-amino-4-thiazolyl)-2-methoxy-iminoacetyl)amino]-ceph-3-eme-4-carboxylic acid, sodium salt) (CTX) is a broad spectrum third-generation cephalosporin antibiotic used to treat both gram-positive and gram-negative bacterial infections. It works by binding to one or more of the penicillin-binding proteins and thereby inhibits bacteria's cell wall synthesis (Luthy et al., 1979). With this background, the present study aimed at evaluating the efficacy of GE and CTX combination against the biofilm formation and the virulence of *S. epidermidis* and MRSA.

2. Materials and methods

2.1. Geraniol and cefotaxime

Geraniol was purchased from Sigma-Aldrich, St. Louis, MO, USA (Catalogue no. 163333) and cefotaxime from Hi-media, Mumbai, India. Stock solution of geraniol and cefotaxime were separately prepared in ethanol and MilliQ water, respectively and stored at 4 °C. The required/working concentrations were prepared from the stock solution.

2.2. Bacterial strain and culture conditions

S. epidermidis (ATCC 35984) and methicillin-resistant *S. aureus* (ATCC 33591) were used in this study. The test pathogens were maintained in Tryptic Soy Agar (TSA) (Hi-Media, Mumbai, India) and cultured in Tryptic Soya Broth (TSB). For biofilm assay, 1% sucrose was used along with TSB for inducing the biofilm formation. For standard cell suspension, an overnight culture of the test pathogen was adjusted to 0.4 OD at 600 nm (1×10^8 CFU/ml).

2.3. Determination of minimum biofilm inhibitory concentration (MBIC)

Assays were performed according to Bakkiyaraj and Pandian (2010). Briefly, 1% of the test pathogen was added to 24 wells polystyrene microtitre plate (MTP) containing 1 ml of TSB + 1% sucrose along with different concentrations of geraniol and cefotaxime separately and also in combination. The cells were then allowed to form biofilm in the wells of MTP at 37 °C for 24 h. After incubation, the planktonic cells were removed and the biofilm adhered on the wells were washed twice with Phosphate buffered saline (PBS, pH 7.4) and then stained with crystal violet (0.4% w/v) solution. The adhered stain in the biofilm cells was eluted with 95% ethyl alcohol and quantified at OD_{570nm} by UV-visible spectrophotometer (Hitachi U-2800, Tokyo, Japan). The MBIC was determined as the least concentration of the combination that shows maximum reduction in the biofilm formation of *S. epidermidis* and MRSA.

2.4. Ring biofilm inhibition assay

The effect of GCC on ring biofilm formation was assessed by growing test pathogens in glass tubes containing 2 ml of TSB + 1% sucrose supplemented with or without GCC at 37 °C for 24 h with shaking at 180 rpm. Following incubation, the tubes were stained with crystal violet solution and photographed (Sethupathy et al., 2017).

2.5. XTT assay

The XTT [2,3-bis(2-methoxy-4-nitro-5-sulphophenyl)-2H-tetrazolium-

5-carboxanilide] reduction assay was performed to determine the metabolic activity of the viable cells (Sivasankar et al., 2016). The untreated control and GCC treated MRSA cells were prepared as described in section 2.3. The untreated and GCC at MBIC treated cells in the MTP wells were washed with PBS and resuspended with the same in equal volume. Exactly, 25 µl of freshly prepared XTT-menadione solution containing XTT (Sigma Aldrich, St. Louis, MO, USA) and menadione (Hi-Media, Mumbai, India) was prepared in the ratio of 12.5:1. The mixture was added to the 200 µl of control and treated cell suspensions and incubated at 37 °C for 8 h in the dark. After incubation, the cells were removed by centrifugation and the supernatant was read at OD_{490nm}. Sterile PBS incubated along with XTT-menadione mixture was used as a blank.

2.6. In situ microscopic visualization

2.6.1. Light microscopic analysis

The efficiency of GCC in the biofilm formation of test pathogens was qualitatively assessed using light microscope by following the method of Bakkiyaraj and Pandian (2010). The test pathogens were incubated along with glass slides (1 × 1 cm) in the wells of MTP containing 1 ml of TSB and 1% sucrose at 37 °C for 24 h in the presence and the absence of GCC. After incubation, the slides were washed with sterile PBS and stained with crystal violet (0.4% w/v). The excess stains in the slides were washed and air dried. The processed slides were further visualized in light microscope (Nikon Eclipse Ti 100, Tokyo, Japan) at 400 × magnification.

2.6.2. Confocal laser scanning microscopic (CLSM) analysis

For CLSM analysis, the biofilms were allowed to form on glass slides as mentioned above. The biofilms on the control and treated slides were washed with sterile PBS and stained with acridine orange (0.1% w/v) solution. The stained biofilms in the slides were imaged under CLSM (LSM 710, Carl Zeiss, Oberkochen, Germany). In addition, biofilm biovolume, average thickness and surface to volume ratio of the biofilm formed in control and treated samples (z-stack images) were analyzed *in silico* using COMSTAT software (kindly gifted by Dr. Claus Sternberg, DTU Systems Biology, Technical University of Denmark) (Kannappan et al., 2017).

2.6.3. Scanning electron microscopic (SEM) analysis

For SEM analysis, the biofilms were allowed to form on glass slides as mentioned above. The biofilms on the control and treated slides were washed with sterile PBS and fixed with 2.5% glutaraldehyde solution for 3 h in dark. The slides were then dehydrated using ethanol at increasing concentrations (20%, 40%, 60%, 80% and 100%) for 2 min in each case. The dehydrated slides were sputter coated by gold and examined under SEM (VEGA 3 TESCAN, Czech Republic) (Kannappan et al., 2017).

2.7. Mature biofilm disruption assay

The ability of GCC in inhibiting the preformed biofilms of the test pathogens were assessed using CLSM. The test pathogens were allowed to form biofilm on the 1 × 1 cm glass slide as described above. At the end of incubation, the glass slides were washed in sterile PBS and transferred to a fresh MTP containing TSB along with GCC at different concentrations (MBIC, 2 × MBIC and 3 × MBIC) and incubated at 37 °C for 24 h. Slides were washed, incubated in acridine orange (0.1% w/v) solution for 5 min and washed again. The stained biofilms in the slides were imaged under CLSM (LSM 710, Carl Zeiss, Oberkochen, Germany) (You et al., 2007).

2.8. Quantification, extraction and characterization of EPS

EPS extraction was done according to Badireddy et al. (2008),

Table 1
List of primers used for real time PCR analysis.

Gene	Nucleotide sequence of primers (5' - 3')		Reference
	Forward primer	Reverse primer	
<i>altE</i>	ATAGAAACGGTGTGGGACGT	ACCTGCACCCCAAGATAAGT	Used in this study
<i>rplU</i>	TTGTAGGTGGCGACTCAGTT	ATGGTTGACGATGGCCTTTT	Used in this study
<i>bhp</i>	TGATGACAAGCGAACGACAA	TGGTGTGGACTCGTAGCTT	Used in this study
<i>ebh</i>	CTAAAGGAACATGGGCAGGC	AAACACCCAGTTGCTAGGA	Used in this study
<i>aap</i>	GGGCAAACGTAGACAAGGTC	GCTTTCGCTTCATGGCTACT	Used in this study
<i>sdrG</i>	GTGACTTGCCTCTGAAAAA	TCCGGTGTTCGAATGTAAT	Used in this study
<i>sdrF</i>	TGAAAAAGAGAAGACAAGAACCA	GATTGCTTCAGCCGCTTTA	Used in this study
<i>sea</i>	ATGGTGCTTATTATGGTTATC	CGTTTCCAAGGTACTGTATT	Kannappan et al. (2017)
<i>gyrB</i>	GGTGCTGGGCAAATACAAGT	TCCCACTAAATGGTGCAA	Sethupathy et al. (2017)
<i>fnbA</i>	ATCAGCAGATGTAGCGGAAG	TTAGTACCGCTCGTTGTCC	Kannappan et al. (2017)
<i>fnbB</i>	AAGAAGCACCGAAAACTGTG	TCTCTGCAACTGCTGTAACG	Kannappan et al. (2017)

where the test pathogens were grown in the presence and the absence of GCC at 37 °C for 24 h. After incubation, the cells and cell free culture supernatants (CFCS) were collected separately by centrifugation at 10,000 rpm for 10 min. CFCS residuals were removed by washing the cell pellets twice with PBS after which the latter were incubated along with isotonic buffer (10 mM Tris/HCl pH 8.0 containing 10 mM EDTA and 2.5% NaCl) at 4 °C for 24 h. After incubation, the cell suspension was vortexed for 10 min centrifuged at 10,000 rpm for 10 min. The supernatant with cell bound EPS was mixed with CFCS followed with three volumes of ice cold acetone and stored at 4 °C for 24 h for the precipitation of cell free and cell bound EPS. Further, EPS was separated by centrifugation at 10,000 rpm for 10 min and finally, the extract was dried under vacuum evaporator (Christ Alpha 2–4 LD plus, SciQuip Ltd, Wem, UK).

The extracted EPS was subjected to FT-IR analysis to observe the changes upon treatment with the GCC. Briefly, 2 mg of extracted EPS was added to 100 mg of potassium bromide (KBr) to prepare the KBr pellet. The infrared spectra for the KBr pellet were recorded with FT-IR system (Nicolet™ iS5, Thermo Scientific, Madison, WI, USA). A total of 64 scans were taken with 4 cm⁻¹ resolution at a range of 4000–400 cm⁻¹. The IR spectra were plotted as absorbance and analyzed using OMNIC software (Schmitt and Flemming, 1998).

2.9. Slime production

To determine the slime production, phenotypic method Congo red agar (CRA) plate assay was performed. CRA plates were prepared as mentioned earlier along with and without GCC (Freeman et al., 1989). To visualize the effect of slime production, the test pathogens were streaked on the GCC free and GCC incorporated CRA plates and incubated at 37 °C for 24 h.

2.10. Quantitative assessment of carotenoid pigment production in MRSA

The untreated control and GCC treated MRSA cells were prepared as described in section 2.4. After incubation, the control and treated cells were collected separately and visually observed for staphyloxanthin inhibition and photographed. Carotenoid extraction was carried out according to the method of Pelz et al. (2005). The bacterial cell pellet was resuspended in ethanol and stored at 40 °C for 10 min. The ethanol was then collected by centrifugation at 12000 rpm for 10 min. The procedure was done repeatedly using pellet until the no visible pigment was obtained. The resulting ethanol was concentrated and the crude pigment mixed with ethyl acetate/1.7 M aqueous sodium chloride (1:1 v/v). The aqueous layer was repeatedly extracted with ethyl acetate until the aqueous layer became colourless. The organic layer was then evaporated to dryness. The whole procedure was done at room temperature and in darkness. Further, the carotenoid was quantitatively measured using ethyl acetate solution. The absorbance were taken for

4,4'- diaphytoene (286 nm); 4,4'-diaponeurosporene (435 nm); 4,4'-diaponeurosporenic acid (455 nm); and b-D-glucopyranosyl 1-O-(4,4'-diaponeurosporene-4-oate)-6-O-(12-methyltetradecanoate) (staphyloxanthin) (462 nm). Ethyl acetate was used as a blank.

2.11. H₂O₂ sensitivity assay

The control and GCC treated cells of *S. epidermidis* and MRSA were prepared as described in section 2.4. The control and treated cells were swabbed on the TSA plates. Further, the swabbed plates were placed with sterile disc on the middle containing 20 µl of 30% H₂O₂. After incubation at 37 °C for 24 h, the plates were observed for zone of inhibition (Liu et al., 2005).

2.12. Whole blood sensitivity assay

The control and GCC treated cells were prepared as described in section 2.4. The cell density of control and treated cultures of *S. epidermidis* and MRSA were adjusted to McFarland standard number 2.0. Three volumes of freshly drawn blood (heparinized) was mixed with 1 volume of the culture and incubated at 37 °C for 3 h with agitation at 160 rpm. After incubation, the samples were enumerated for viable cells (Liu et al., 2005).

2.13. Real time PCR analysis

Total RNA was isolated from the cells of *S. epidermidis* and MRSA treated with and without GCC using Trizol method. The extracted mRNA was converted into cDNA using High Capacity cDNA Reverse Transcription Kit (Applied Biosystems Inc., USA). Quantitative real-time PCR analysis (qPCR) was performed on an Applied Biosystems thermal cycler using the Power SYBR Green PCR Master Mix (Applied Biosystems Inc., USA). The data set was normalized with reference gene of MRSA (*gyrB*, gyrase) and *S. epidermidis* (*rplU*, ribosomal protein). *S. epidermidis* gene specific primers used in this study were designed using Primer3 and were synthesized by Sigma-Aldrich. The amplification of the target genes using designed primers were validated using *in silico* and conventional PCR analysis and their sequences listed in Table 1. In response to GCC, relative expression of the target genes were quantified using gene-specific primers (Table 1) with the help of standard formula described by Yuan et al. (2006).

2.14. In vivo biofilm formation assay

The antibiofilm activity of test pathogens was assessed using *Caenorhabditis elegans* as a live model organism. Briefly, the test pathogens at standard cell suspension (1 × 10⁸ cells/ml) were added to the MTP containing nematodes (n = 10) in M9 buffer along with and without GCC at MBIC. The experiment left undisturbed for 24 h at 20 °C.

Following incubation, the nematodes infected with the test pathogens in the presence and the absence of GCC were washed thrice with M9 buffer containing 0.1% acridine orange solution. The stained nematodes were again washed with M9 buffer to remove excess stain. The washed nematodes were placed on the glass slides with 0.01% sodium azide solution (for immobilization) and visualized under CLSM, where the fluorescence intensity was directly proportional to the rate of bacterial colonization (Jansen et al., 2002).

2.15. CFU assay

The effect of GCC on the internal colonization of the test pathogens inside *C. elegans* was determined using CFU assay wherein, nematodes were infected with test pathogens in the presence and absence of GCC as mentioned in subsection 2.14. Initially, the nematodes were washed with 0.5 µg/ml tetracycline to kill the bacterial cells adhered to the external surface of nematodes. The internalized bacteria were extracted by vortexing the nematodes in the silicon carbide (0.4 g) solution. The colony forming units of the released bacteria were quantified using spread plate method.

2.16. Statistics

All the experiments were done in experimental triplicate for thrice. Values were expressed in mean ± standard deviation (SD) and the statistical analysis was done using SPSS package (SPSS v20.0; SPSS Inc., Armonk, NY, USA). One way ANOVA and student-t tests were used to compare the control and treated samples. *P* was set at < 0.05 to determine the significant level.

3. Results

3.1. Effect of GE and CTX combination (GCC) on biofilm formation and viability

Initially, different concentrations of GE (50, 75, 100 and 125 µg/ml) and CTX (1 and 2 µg/ml) were assessed individually to determine the MIC against *S. epidermidis* and MRSA. The *in vitro* result indicated that GE has neither antibacterial nor antibiofilm activity at the tested concentrations, whereas CTX showed growth inhibition at the highest concentration (10 µg/ml) tested (Fig. 1A and B). So, CTX at sub-inhibitory concentration (2 µg/ml & 1 µg/ml) was used for assessing its combinatorial activity along with GE. In the present study, it was observed that the combination of GE (100 µg/ml) and CTX (2 µg/ml) effectively reduced the biofilm formed by the test pathogens compared to that of individual compound and untreated control without any reduction in the planktonic growth of the *S. epidermidis* and MRSA (Fig. 1C and D). Further, visualization of biofilm formed by the pathogens (biofilm ring assay) on test tubes evident the antibiofilm potential of GCC. Hence, this combination (100 µg of GE and 2 µg of CTX) was fixed as MBIC and the same was used for further assays. To be an ideal antibiofilm agent, it should target the biofilm formation and not metabolic activity of the cell. To substantiate the fact, XTT assay was done. The XTT result unveiled the non-antibacterial property of GCC, and thus, signifies its potential against the biofilm formation of test pathogens (Fig. S1).

3.2. Microscopic observation of biofilm formation

The antibiofilm potential of GCC at its MBIC was further confirmed using light, confocal laser scanning and scanning electron microscope analysis. Light and CLSM micrographs clearly showed the reduction in the biofilm formation of the test pathogens in the presence of GCC at its MBIC (Fig. 2A and B). The results of CLSM analysis were further validated using COMSTAT analysis. As seen in Fig. 2B, the parameters like biofilm biomass and average thickness were highly reduced with

increase in surface to volume ratio (Table 2). Further, the observation of SEM micrographs confirms the loss of microcolony and multi-layered biofilm architecture formation upon GCC treatment whereas control slide showed a typical feature of staphylococcal biofilms with multi-layered adherent cells (Fig. 2C).

3.3. Effect of GCC on EPS

FT-IR characterization was done to observe the changes in EPS produced by the test pathogens upon GCC treatment. The results of FT-IR analysis validated the variations in the peaks corresponds to amide I (1700–1600 cm^{-1}) and amide II (1600–1500 cm^{-1}) regions associated with proteins upon GCC treatment (Fig. 3A and B).

3.4. Effect of GCC on slime production

The ability of GCC to inhibit the slime production in staphylococci was qualitatively assessed using congo red agar (CRA) medium. Classical black colour formation with consistent dry crystalline colonies is the typical feature of slime producing biofilm forming staphylococci on CRA medium and was evident from the control CRA plates. The results of the CRA assay clearly demonstrated that the GCC at MBIC was potent enough to suppress the slime production in the test pathogens when compared to the untreated controls of the test pathogens (Fig. 3C).

3.5. GCC alters the staphyloxanthin pigment production and not the antioxidant potential of MRSA

Since staphyloxanthin protects the MRSA cells from the effect of host immune responses and oxidative stresses, GCC at MBIC was assessed for its ability on the staphyloxanthin and its derivative production in MRSA. Even though a visual reduction in the pigment production was observed when the MRSA cells treated with GCC at MBIC (Fig. 4A), the GCC treated cells showed insignificant results when exposed to H_2O_2 (Fig. 4B).

3.6. Effect of GCC on the survival of test pathogens in whole blood

The survival of test pathogens in healthy human blood was assessed by blood sensitivity assay. The results showed a significant decrease in the survival of *S. epidermidis* and MRSA to a level of $3 \pm 0.76 \times 10^5$ and $4 \pm 0.61 \times 10^5$ cells, respectively upon GCC treatment whereas untreated controls of *S. epidermidis* and MRSA showed a survival rate of $23 \pm 2.16 \times 10^5$ and $14 \pm 1.02 \times 10^5$ cells, respectively in healthy human blood (Fig. 4C).

3.7. Mature biofilm disruption assay

Preformed biofilms resist the penetration of antimicrobials and host immune responses and thereby aid the everlasting chronic bacterial infections in healthcare settings. The results of CLSM analysis clearly revealed that GCC have no significant effect in dislodging the preformed biofilms of test pathogens at the tested concentrations (Fig. 5A).

3.8. GCC modulates the expression of surface adhesins genes

To find out the effect of GCC on candidate genes, qPCR was performed. Since GCC was not active on mature biofilms, expression of few genes responsible for the surface adhesion of *S. epidermidis* (*aap*, *sdrG*, *sdrF*, *bhp*, *ebh*, *altE*) and MRSA (*fnbA*, *fnbB*, & *clfA*) were studied. The expression levels of GCC treated cells were compared with control and normalized to one. The data of expression analysis displayed significant down regulation in the genes responsible for surface adhesion. Further, the gene responsible for virulence factor production in MRSA such as Staphylococcal enterotoxin A (*sea*) was also down regulated upon GCC

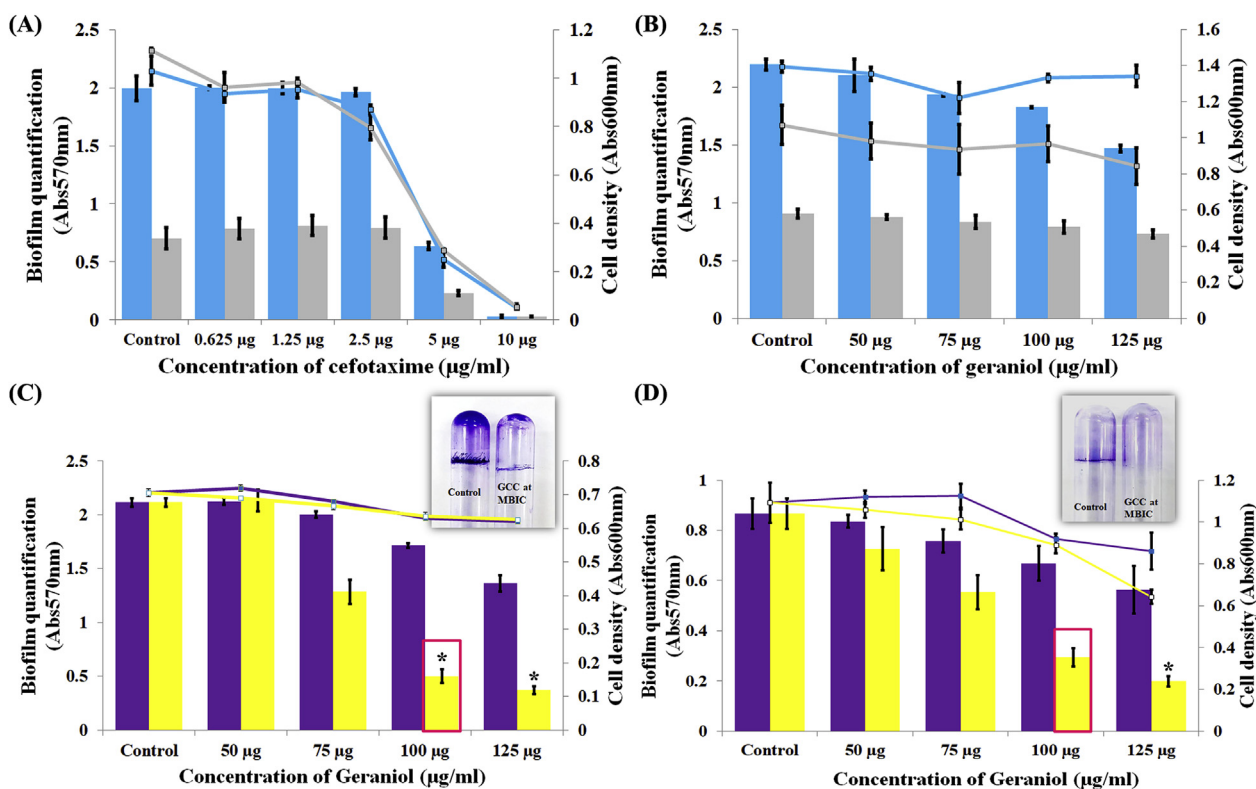


Fig. 1. Effect of geraniol (A) and cefotaxime (B) alone on the biofilm formation and growth of *S. epidermidis* (■) and MRSA (■). Effect of cefotaxime at 1 µg/ml (■) and 2 µg/ml (■) in combination with geraniol at different concentration (50, 75, 100 and 125 µg/ml) on biofilm formation and the growth of *S. epidermidis* (C) and MRSA (D). Mean values of triplicate independent experiments and SD are shown. * indicates significance at $p \leq 0.05$. Geraniol at 100 µg/ml and cefotaxime at 2 µg/ml reduced the maximum biofilm formed by the test pathogens. Hence, this concentration of GCC was fixed as MBIC. Bar represents the biofilm formation and line represents the growth of the test pathogens. Inlet images (in Fig. 1C and D) showing the potential of GCC at MBIC against test pathogens on ring biofilm formation in test tubes.

treatment (Fig. 5B).

3.9. *In vivo* evaluation of the potentials of GCC using *C. elegans* as model organism

3.9.1. *In vivo* biofilm formation assay using *C. elegans*

Further to confirm the antibiofilm activity of GCC, internal colonizing ability of the test pathogens in *C. elegans* was assessed in the presence and the absence of GCC using CLSM. Nematodes challenged with test pathogens exhibited an increased colonization with distorted pharynx and internal hatching of eggs. In contrast, nematodes challenged with GCC and test pathogens cells showed reduction in the internal colonization with healthy pharynx (Fig. 6A).

3.9.2. CFU assay

Further to confirm the microscopic results, internalization of the test pathogens were quantitatively assessed using CFU assay. As shown in Fig. 6b, untreated cells of *S. epidermidis* and MRSA colonized in nematodes to a level of $26.00 \pm 2.64 \times 10^2$ and $50.00 \pm 2.00 \times 10^4$ CFU/worm, respectively. Meanwhile, supplementation with GCC significantly reduced the colonization of *S. epidermidis* and MRSA in nematodes to CFU of $16.67 \pm 1.15 \times 10^2$ and $23.00 \pm 6.08 \times 10^4$ CFU/worm, respectively. The results of the internal colonization studies suggested the antibiofilm potential of GCC against *S. epidermidis* (Fig. 6B).

4. Discussion

The biofilm mediated antimicrobial tolerance poses a serious threat in nosocomial settings. The ability of bacterial pathogens to form

biofilms in the nosocomial settings lead to hard-to-treat infections (Davies, 2003). Although the scientific communities are continuously involved in developing new treatment approaches to treat biofilm mediated infections, the successful treatment strategies are much scarce. However, the polytherapy approach is gaining interest in controlling the biofilm mediated infections as it has multi-dimensional mode of actions and prevents the development of antimicrobial resistance (Bulusu et al., 2016). In the present study, the polytherapy approach using geraniol and a third-generation cephalosporin antibiotic, cefotaxime, was assessed for its *in vitro* and *in vivo* biofilm inhibitory potential against *S. epidermidis* ATCC 35984 and MRSA ATCC 33591.

In the present study, it was observed that the combination of geraniol (100 µg/ml) and cefotaxime (2 µg/ml) (GCC) effectively inhibited the biofilm formed by the test pathogens compared to that of individual compound or untreated control without inhibiting the growth. Similar to this study, there are plethora of works reported the efficacy of phytocompounds upon combination with antibiotics against several nosocomial pathogens even at its lowest concentration. Chung et al. (2011) have studied the synergistic potentials of pentacyclic triterpenoids (α -amyrin, betulinic acid and betulinolaldehyde) and antibiotics (methicillin and vancomycin) against *S. aureus*. Similarly, the use of combination therapy was highlighted in the very recent work of Asli et al. (2017), where the combination of chitosan along with macrolide class of antibiotic (tilmicosin) reduced the usage of both the compound by 2–8 times against *S. aureus* growth and biofilm formation. To be a good antibiofilm agent, it should target the biofilm formation and not the metabolic activity of the cell. To substantiate the fact, subsequent XTT assay for the GCC unveiled its non-antibacterial property, and thus, signifies the antibiofilm efficacy of GCC. Development of characteristic

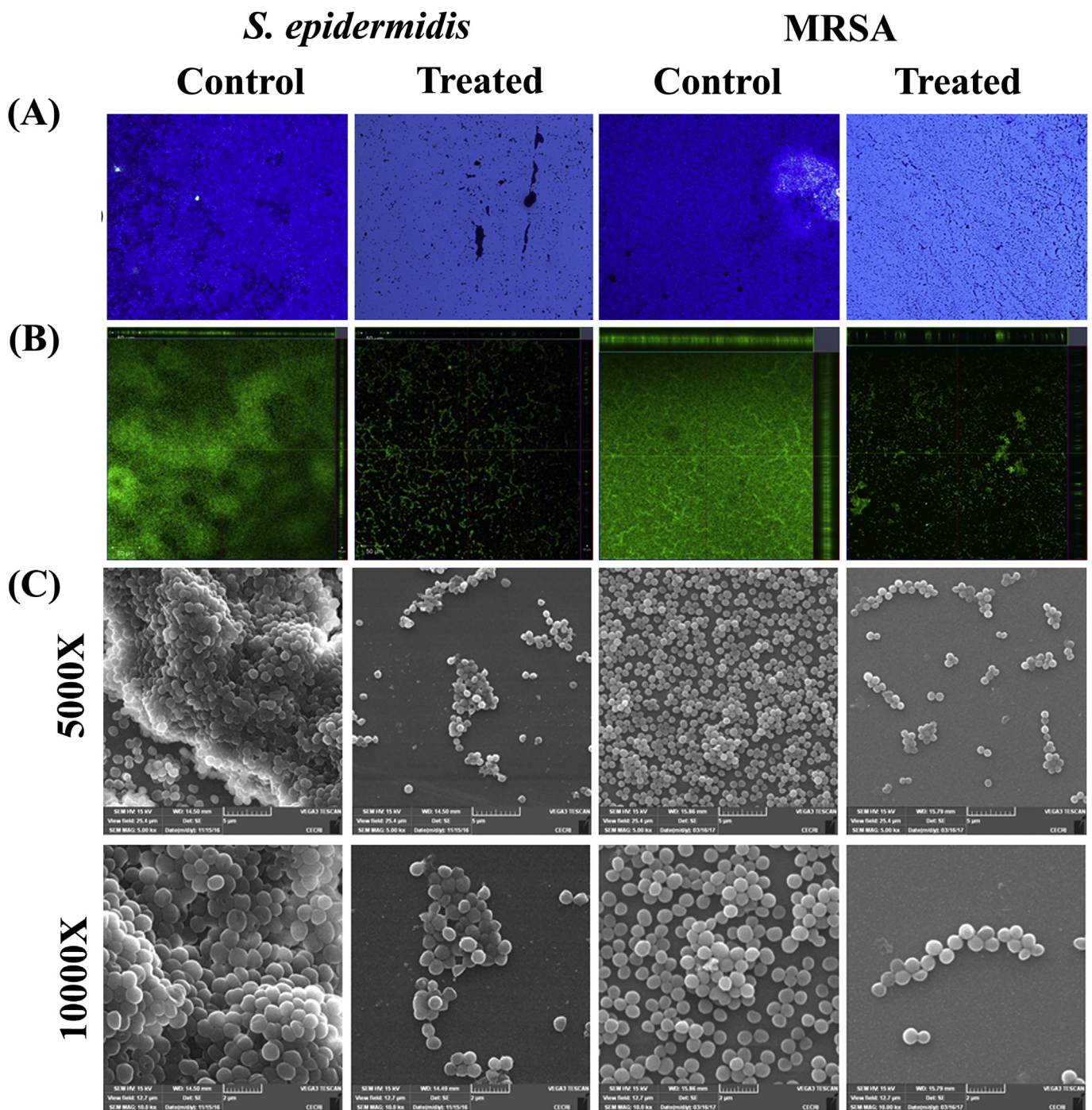


Fig. 2. Microscopic observation of biofilms formed by test pathogens on glass slides in the presence and absence of GCC at MBIC. Light (A), CLSM (B) and SEM analysis (C).

Table 2
COMSTAT analysis of GCC treated (at MBIC) and untreated samples of *S. epidermidis* and MRSA.

	<i>S. epidermidis</i> ATCC 35984		MRSA ATCC 33591	
	Untreated control	GCC treated	Untreated control	GCC treated
Biofilm Biovolume ($\mu\text{m}^3/\mu\text{m}^2$)	72.45	20.58	49.79	35.63
Max. Thickness (μm)	70.81	19.6	47.30	33.85
Surface to volume ratio ($\mu\text{m}^2/\mu\text{m}^3$)	0.01826	0.0533	0.02479	0.03277

biofilm architecture is a crucial step in staphylococcal pathogenesis. Further, microscopic visualization biofilms using light, CLSM and scanning microscopy ascertained the changes exerted by GCC and thus the results of the microscopic analyses corroborate well with the results of biofilm biomass quantification assay. Result of the microscopy analyses obtained is superior to the recent findings of [Vadekeetil et al. \(2016\)](#) where an antibiofilm compound, ajeone (2500 mg/ml) in combination with an antibiotic ciprofloxacin (60 $\mu\text{g}/\text{ml}$) inhibits the *in vitro* biofilm formation *pseudomonas aeruginosa* and further highlighted the *in vivo* potential of this combination (ajeone at 25 mg/kg and ciprofloxacin at 30 mg/kg) in clearing the *P. aeruginosa* mediated acute pyelonephritis infections in mice model.

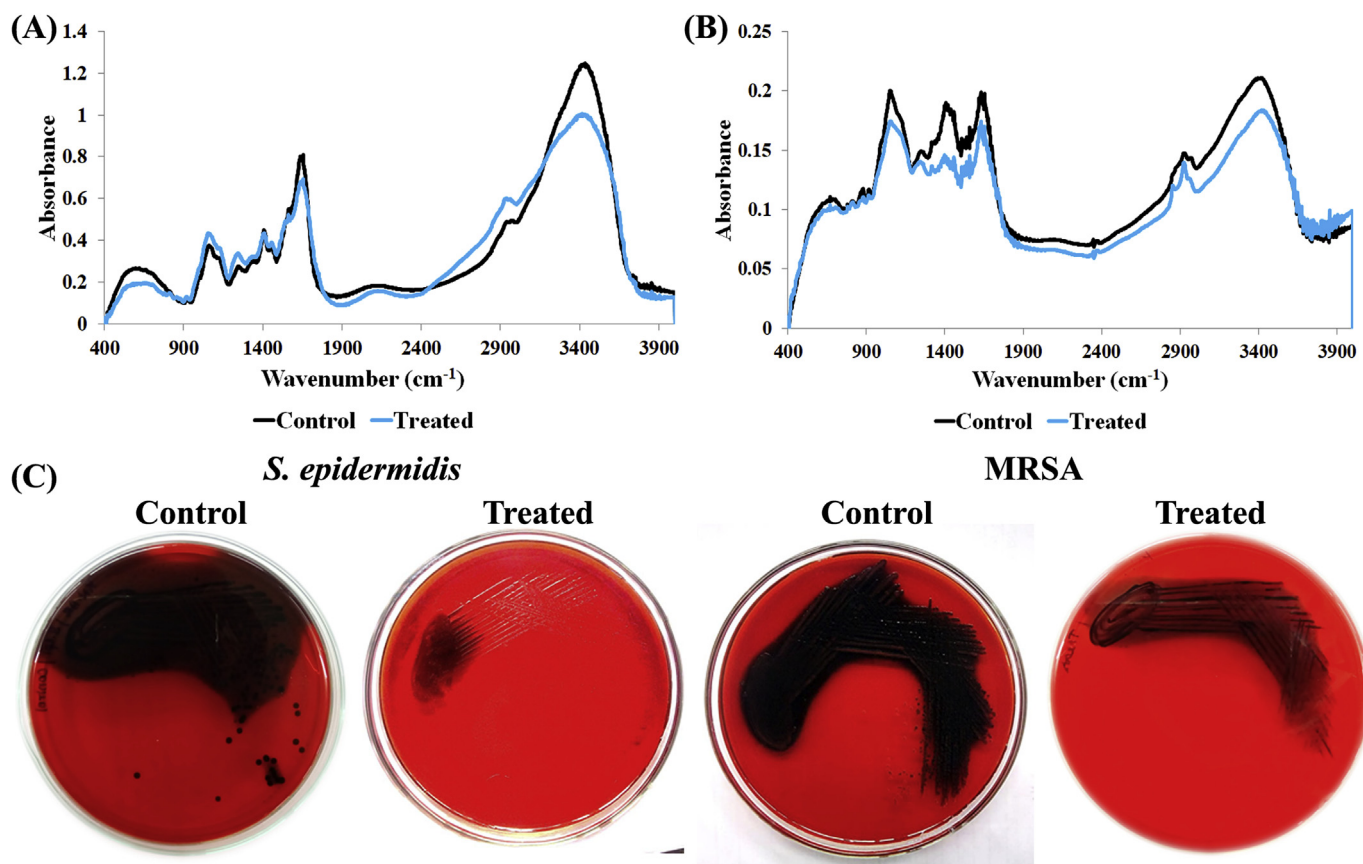


Fig. 3. FT-IR spectra of EPS isolated from *S. epidermidis* (A) and MRSA (B) treated with and without GCC. The level of slime synthesis by the test pathogens in CRA plates supplemented with and without GCC at MBIC (C).

The persistence of biofilm is attributed to its matrix made up of EPS, which contains proteins, polysaccharides and eDNA (Flemming and Wingender, 2010). EPS act as a protective barrier against the entry of the antimicrobials and other host defense mechanisms (Fux et al., 2005). Thus, it is suggested that suppressing the EPS synthesis could weaken the biofilm architecture and increases the pathogen susceptibility to the host immune responses. Similar action was observed when the test pathogens were treated with GCC and it was more evident through scanning microscopic observations and FT-IR analysis. The amide I ($1700\text{--}1600\text{ cm}^{-1}$) and amide II ($1600\text{--}1500\text{ cm}^{-1}$) regions contain the information on structural properties of proteins in EPS. The amide I band of protein region exhibits β -sheet structure and most sensitive to conformational changes (Omoike and Chorover, 2004). EPS proteins with this secondary structure play a vital role in initial attachment and biofilm formation. FT-IR analysis of EPS from GCC treated culture showed a reduction in the IR signal corresponds to the region of amide I of protein region ($1700\text{--}1600\text{ cm}^{-1}$) and which could be attributed to the conformational changes in EPS proteins and thereby decrease in the biofilm formation. The result of FT-IR is generally analogous to another report on humic acid on the adhesion of *Bacillus subtilis*, suggesting that the observed result was due to the conformational changes in amide I and amide II regions of surface proteins (Hong et al., 2015).

Similar to EPS, slime plays an important role in host tissue colonization and provides better fortification from phagocytosis and opsonization (Ammendolia et al., 1999). Recent reports evidenced the effect of *Staphylococcus* sp. biofilm inhibitors on slime production (Chu et al., 2016; Kannappan et al., 2017; Sethupathy et al., 2017). Results of CRA plate assay revealed the efficiency of GCC in suppressing the slime production in the test pathogens. In addition to EPS and slime production, MRSA produces several virulence factors that enable the

survival of this pathogen in the presence of antimicrobial agents and host immune responses. Staphyloxanthin, a carotenoid pigment with antioxidant potential, is responsible for the MRSA survival in the presence of oxidants (Pelz et al., 2005). Hence, it is suggested that inhibition of staphyloxanthin make the MRSA cells susceptible to the host immune responses and antimicrobial agents. Visualization of MRSA cells clearly inferred that GCC inhibits the staphyloxanthin pigment production. Further, the quantitative results showed that GCC inhibits the pigment production significantly to a measurable level at $OD_{462\text{nm}}$. Moreover, the treatment with GCC inhibits the precursors like 4,4'-diaponeurosporene and 4,4'-diaponeurosporenic acid. In contrast to other pigments, GCC treated cells shown to produce a higher level of 4,4'-diapophytoene. The results of the present study corroborate well with the results of Leejae et al. (2013), in which rhodomlyrtone suppresses the synthesis of staphyloxanthin pigment and its intermediates in MRSA with increased 4,4'-diapophytoene production. They claimed that the acquired result would be due to the compound rhodomlyrtone which could induce the CrtM enzyme activity. Similarly, Lee et al. (2013) reported that indole and its derivatives act as an antiviral agent by lowering the production of staphyloxanthin pigment in MRSA, which in turn enhance the survival of *C. elegans* during MRSA infection.

Staphyloxanthin reduces the susceptibility of MRSA towards the oxidative stress and host immune responses. Though several natural compounds were reported to inhibit the staphyloxanthin pigment production in MRSA (Sakai et al., 2012), the efficacy of those compounds towards oxidative stress and host immune responses still remain at infancy. The results showed that treatment with GCC sensitized the MRSA cells to the action of host neutrophil-based killing when compared to the control cells. The result obtained in the present study corroborates well with the recent findings of Sethupathy et al. (2017), where MRSA cells showed a reduced level of staphyloxanthin pigment

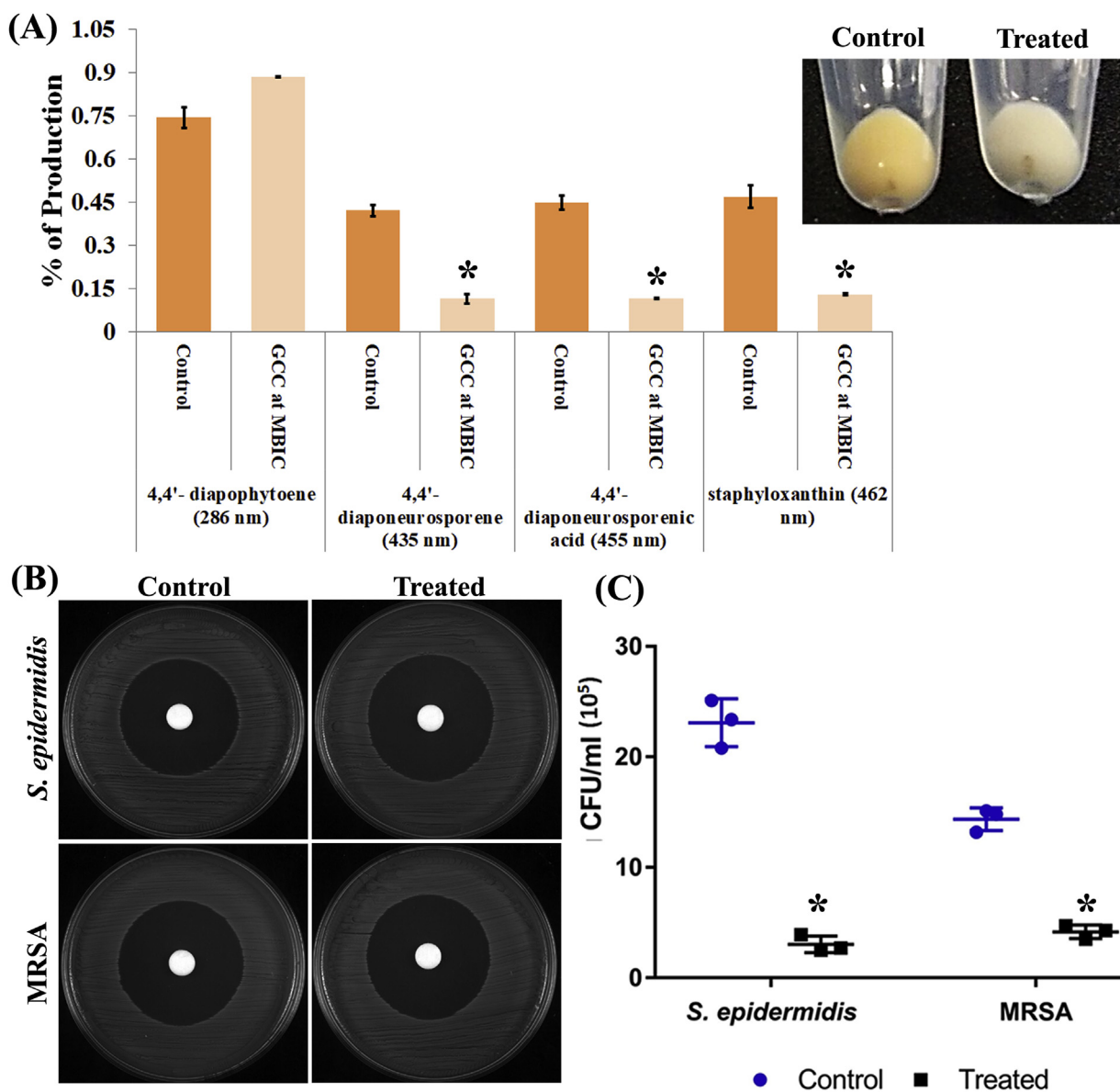


Fig. 4. Effect of GCC at MBIC on the carotenoid pigment production in MRSA (A), GCC treatment affects the ability of test pathogens survival in the presence of H₂O₂ (B) and whole blood (C). Mean values of triplicate independent experiments and SD are shown. * indicates significance at $p \leq 0.05$. Inlet image (in Fig. 4A) showing the reduction in staphyloxanthin pigment production in MRSA cells upon treatment with GCC.

production and survival rate in whole blood sensitivity assay upon treatment with L-Ascorbyl 2,6-dipalmitate. In contrast to the results of staphyloxanthin biosynthesis and whole blood survival assay, GCC treated cells have no significant effect on its survival in the presence of H₂O₂.

Preformed biofilms are the real players in the biofilm mediated infection, which causes much more complications in healthcare settings to treat (Fux et al., 2005). As GCC have no significant effect on eradicating the mature biofilms of the test pathogens, qPCR analysis was done for the genes involved in the initial attachment. The first step in staphylococcal adhesion to host extracellular matrix is mediated by cell wall anchored (CWA) proteins called microbial surface components recognizing adhesive matrix molecules (MSCRAMMs). Clumping factor (ClfA) and fibronectin-binding protein (FnbA) are CWA surface proteins which attaches to the fibrinogen and fibronectin, respectively (Cucarella et al., 2002). Similarly, *sdrG* and *sdrF*, a member of serine aspartate protein repeats (*sdr*), is necessary for the sufficient attachment of *S. epidermidis* to the surface coated with fibrinogen. The Bhp protein has been proposed to endorse primary attachment to form

biofilm, whereas Aap is required for the accumulation that results in visible biofilm (Davis et al., 2001). Hence, we assessed the transcripts level of those CWA proteins in *S. aureus* and *S. epidermidis* as an index of biofilm formation. As anticipated, qPCR analysis resulted in the down-regulation of *clfA*, *fnbA*, *sdrG*, *sdrF*, *bhp* and *aap* transcript levels upon GCC treatment. In a recent study, Schommer et al. (2011) reported that the PIA-, Embp- and Aap-dependent biofilms resistant the phagocytosis activity due to their ability to inhibit NF- κ B activation and interleukin-1 β (IL-1 β) production. The inability of *S. epidermidis* to survive in the whole blood might be due to the effect of GCC on *aap* production. Furthermore, GCC reduces the expression of virulence genes like *sea* in MRSA. In addition to its anti-adherence potential, down-regulation of the virulence gene like *sea* validates that GCC targets not only the initial attachment of the biofilm cells but also other toxins production of the test pathogens.

Since GCC inhibits the widely recognized pathogenic traits of *Staphylococcus* sp., which drives us to study *in vivo* the anti-adherence potential of GCC using simple, free-living animal model. *C. elegans* is a simple *in vivo* model organism and possesses several experimental

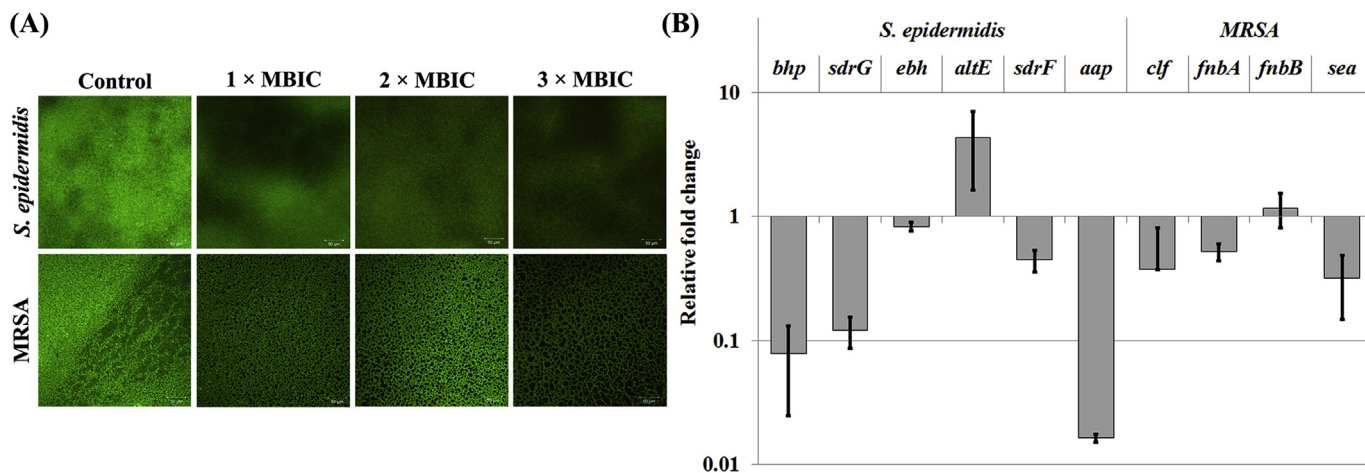


Fig. 5. CLSM analysis showing the non-inhibitory effect of GCC on the preformed biofilms of the test pathogens (A). Gene expression analysis represents transcription level of candidate genes associated with initial attachment of the test pathogens to form biofilms in response to the MBIC of GCC (B). Mean values of triplicate independent experiments and SDs are shown.

advantages to study the bacterial pathogenesis (Couillault and Ewbank, 2002). It is progressively recognized as a practical and ethically attractive model system for studying host pathogen interactions. *C. elegans* produces ROS as host protective innate mechanism to counteract bacterial invasion (Chávez et al., 2009). Meanwhile, MRSA produces an antioxidant pigment staphyloxanthin to neutralize the host ROS action. In *in vivo* biofilm formation assay using *C. elegans*, the treatment with GCC reduced the intestinal bacterial colonization in the *C. elegans* and was evidenced from the CLSM analysis. Hence, the result obtained is speculated that interference of staphyloxanthin pigment production by GCC increased the clearance of MRSA colonization in *C. elegans*.

Further, estimation of bacterial burden in the worm was assessed by CFU assay. The results of the internal colonization studies suggested the

potential of GCC against the adherence of *S. epidermidis* to host tissues. In concordance with these findings, ellagic acid (500 µg/ml) and tetracycline (0.312 µg/ml) combination was found to inhibit the biofilm formation of *Propionibacterium acnes* strains and subsequent internal colonization of *P. acnes* cells in *C. elegans* (Sivasankar et al., 2016). Similarly, extract from coral associated actinomycetes showing anti-biofilm activity against *S. aureus* significantly reduced the colonization of *C. elegans* (Bakkiyaraj and Pandian, 2010). Thus, the result of the present study implies that GCC hinders the biofilm formation of *Staphylococcus* spp. thereby aiding the elimination of test pathogen by the host immune system under *in vivo* conditions.

In conclusion, the present work for the first time delineates the combinatorial antibiofilm potential of GE and CTX against *S. epidermidis*

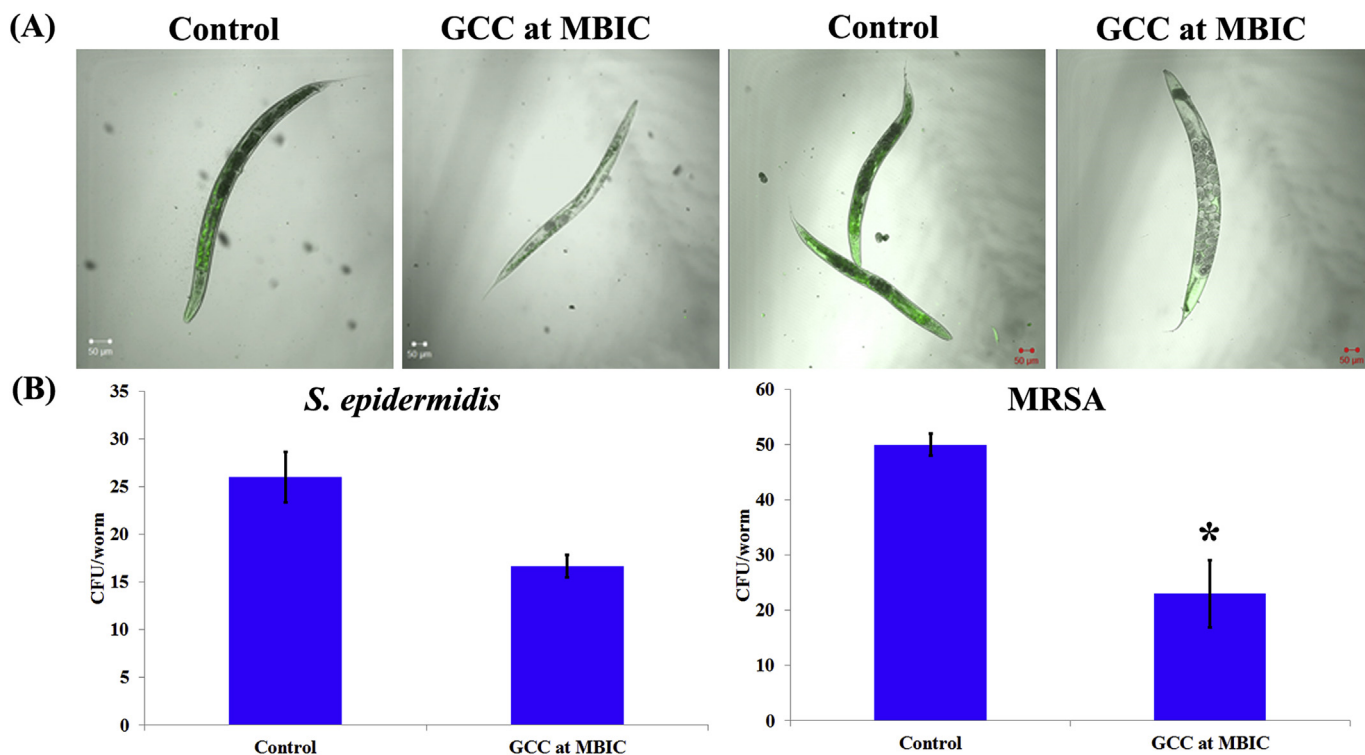


Fig. 6. *In vivo* analysis of *C. elegans*. CLSM micrographs showing the rescuing potential of GCC at MBIC (A). Level of fluorescence is directly proportional to the level of bacterial colonization. Bacterial cell count revealed that GCC at MBIC reduced the bacterial load in *C. elegans* significantly (B). Mean values of triplicate independent experiments and SD are shown. * indicates significance at $p \leq 0.05$.

and MRSA. Significant reduction in the biofilm biomass and slime production validated the antibiofilm potential of GCC. In addition, microscopy analyses and variation in the FI-IR spectra of GCC treated EPS corroborate the results of *in vitro* biofilm inhibition assay. Results of mature biofilm disruption assay and qPCR analysis suggested that GCC targets the initial attachment of the cells to form biofilm. Exposure of test pathogens to GCC reduces the staphyloxanthin pigment production in MRSA and in turn makes the pathogenic cells susceptible to the host immune responses. Further, *in vivo* studies using *C. elegans* suggested the suitability of GCC in controlling the biofilm associated infections of *Staphylococcus* sp.

Conflicts of interest

Authors have no conflict of interest to declare.

Ethical approval

In the present study, healthy human blood was used only for research purposes. The blood sample used in the study was taken by technically trained persons. The use of the sample and experimental methodology was assessed and approved by the Institutional Ethical Committee under the no. IEC/AU/2016/1/6.

Acknowledgment

The authors sincerely acknowledge the computational and bioinformatics facility provided by the Alagappa University, Bioinformatics Infrastructure Facility (funded by DBT, GOI; File No. BT/BI/25/015/2012, BIF). Financial assistance rendered to AR. Kannappan by University Grants Commission in the form of UGC-BSR Fellowship is thankfully acknowledged [grant no. F.25-1/2014-15(BSR)/7-326/2011(BSR)]. The authors thankfully acknowledge the financial support rendered through RUSA – Phase 2.0 [grant no. F. 24-51/2014-U, Policy (TNMulti-Gen), Dept. of Edn., Govt. of India, Dt. 19.10.2018]. The authors also thankfully acknowledge the Department of Science and Technology - Fund for Improvement in S&T Infrastructure (DST-FIST) (grant no. SR/FST/LSI-639/2015(C)), University Grants Commission - Special Assistance Programme - Department Research Support (UGC SAP -DRS-II) (grant no. F.5-1/2018/DRS-II(SAP-II)) and Department of Science and Technology - Promotion of University Research and Scientific Excellence Grant (DST-PURSE) (grant no. SR/PURSE Phase 2/38 (G)) for providing instrumentation facilities.

Transparency document

Transparency document related to this article can be found online at <https://doi.org/10.1016/j.fct.2019.01.008>.

Appendix A. Supplementary data

Supplementary data to this article can be found online at <https://doi.org/10.1016/j.fct.2019.01.008>.

References

Ammendolia, M.G., Di Rosa, R., Montanaro, L., Arciola, C.R., Baldassarri, L., 1999. Slime production and expression of the slime-associated antigen by staphylococcal clinical isolates. *J. Clin. Microbiol.* 37, 3235–3238.

Asli, A., Brouillette, E., Ster, C., Ghinet, M.G., Brzezinski, R., Lacasse, P., Jacques, M., Malouin, F., 2017. Antibiofilm and antibacterial effects of specific chitosan molecules on *Staphylococcus aureus* isolates associated with bovine mastitis. *PLoS One* 12.

Badireddy, A.R., Korpil, B.R., Chellam, S., Gassman, P.L., Engelhard, M.H., Lea, A.S., Rosso, K.M., 2008. Spectroscopic characterization of extracellular polymeric substances from *Escherichia coli* and *Serratia marcescens*: suppression using sub-inhibitory concentrations of bismuth thiols. *Biomacromolecules* 9, 3079–3089.

Bakkiyaraj, D., Pandian, S.K., 2010. *In vitro* and *in vivo* antibiofilm activity of a coral associated actinomycete against drug resistant *Staphylococcus aureus* biofilms.

Biofouling 26, 711–717.

Bulusu, K.C., Guha, R., Mason, D.J., Lewis, R.P.I., Muratov, E., Kalantar Motamedi, Y., Cokol, M., Bender, A., 2016. Modelling of compound combination effects and applications to efficacy and toxicity: state-of-the-art, challenges and perspectives. *Drug Discov. Today* 21, 225–238.

Chávez, V., Mohri-Shiomi, A., Garsin, D.A., 2009. Ce-Duox1/BLI-3 generates reactive oxygen species as a protective innate immune mechanism in *Caenorhabditis elegans*. *Infect. Immun.* 77, 4983–4989.

Chu, M., Zhang, M., Liu, Y., Kang, J., Chu, Z., Yin, K., Ding, L., Ding, R., Xiao, R., Yin, Y., Liu, X., Wang, Y., 2016. Role of Berberine in the treatment of methicillin-resistant *Staphylococcus aureus* infections. *Sci. Rep.* 6, 24748.

Chung, P.Y., Navaratnam, P., Chung, L.Y., 2011. Synergistic antimicrobial activity between pentacyclic triterpenoids and antibiotics against *staphylococcus aureus* strains. *Ann. Clin. Microbiol. Antimicrob.* 10.

Couillault, C., Ewbank, J.J., 2002. Diverse bacteria are pathogens of *Caenorhabditis elegans*. *Infect. Immun.* 70, 4705–4707.

Cucarella, C., Tormo, M.Á., Knecht, E., Amorena, B., Lasa, Í., Foster, T.J., Penadés, J.R., 2002. Expression of the biofilm-associated protein interferes with host protein receptors of *Staphylococcus aureus* and alters the infective process. *Infect. Immun.* 70, 3180–3186.

Davies, D., 2003. Understanding biofilm resistance to antibacterial agents. *Nat. Rev. Drug Discov.* 2, 114–122.

Davis, S.L., Gurusiddappa, S., McCreia, K.W., Perkins, S., Höök, M., 2001. SdrG, a fibrinogen-binding bacterial adhesin of the microbial surface components recognizing adhesive matrix molecules subfamily from *Staphylococcus epidermidis*, targets the thrombin cleavage site in the B β chain. *J. Biol. Chem.* 276, 27799–27805.

Flemming, H.C., Wingender, J., 2010. The biofilm matrix. *Nat. Rev. Microbiol.* 8, 623–633.

Flemming, H.C., Wingender, J., Szewzyk, U., Steinberg, P., Rice, S.A., Kjelleberg, S., 2016. Biofilms: an emergent form of bacterial life. *Nat. Rev. Microbiol.* 14, 563–575.

Freeman, D.J., Falkiner, F.R., Keane, C.T., 1989. New method for detecting slime production by coagulase negative staphylococci. *J. Clin. Pathol.* 42, 872–874.

Fux, C.A., Costerton, J.W., Stewart, P.S., Stoodley, P., 2005. Survival strategies of infectious biofilms. *Trends Microbiol.* 13, 34–40.

Hong, Z., Chen, W., Rong, X., Cai, P., Tan, W., Huang, Q., 2015. Effects of humic acid on adhesion of *Bacillus subtilis* to phyllosilicates and goethite. *Chem. Geol.* 416, 19–27.

Jansen, W.T.M., Bolm, M., Balling, R., Chhatwal, G.S., Schnabel, R., 2002. Hydrogen peroxide-mediated killing of *Caenorhabditis elegans* by *Streptococcus pyogenes*. *Infect. Immun.* 70, 5202–5207.

Jeong, E.-Y., Cho, K.-S., Lee, H.-S., 2012. Food protective effects of *Periploca sepium* oil and its active component against stored food mites. *J. Food Protect.* 75, 118–122.

Kannappan, A., Gowrishankar, S., Srinivasan, R., Pandian, S.K., Ravi, A.V., 2017. Antibiofilm activity of *Vetiveria zizanioides* root extract against methicillin-resistant *Staphylococcus aureus*. *Microb. Pathog.* 110, 313–324.

Kostakioti, M., Hadjifrangiskou, M., Hultgren, S.J., 2013. Bacterial biofilms: development, dispersal, and therapeutic strategies in the dawn of the postantibiotic era. *Cold Spring Harb. Perspect. Med.* 3.

Lebeaux, D., Ghigo, J.-M., Beloin, C., 2014. Biofilm-related infections: bridging the gap between clinical management and fundamental aspects of recalcitrance toward antibiotics. *Microbiol. Mol. Biol. Rev.* 78, 510–543.

Lee, J.H., Cho, H.S., Kim, Y., Kim, J.A., Banksota, S., Cho, M.H., Lee, J., 2013. Indole and 7-benzyloxyindole attenuate the virulence of *Staphylococcus aureus*. *Appl. Microbiol. Biotechnol.* 97, 4543–4552.

Leejae, S., Hasap, L., Voravuthikunchai, S.P., 2013. Inhibition of staphyloxanthin biosynthesis in *Staphylococcus aureus* by rhodomyrone, a novel antibiotic candidate. *J. Med. Microbiol.* 62, 421–428.

Liu, G.Y., Essex, A., Buchanan, J.T., Datta, V., Hoffman, H.M., Bastian, J.F., Fierer, J., Nizet, V., 2005. *Staphylococcus aureus* golden pigment impairs neutrophil killing and promotes virulence through its antioxidant activity. *J. Exp. Med.* 202, 209–215.

Luthy, R., Munch, R., Blaser, J., Bhend, H., Siegenthaler, W., 1979. Human pharmacology of cefotaxime (HR 756), a new cephalosporin. *Antimicrob. Agents Chemother.* 16, 127–133.

Omoike, A., Chorover, J., 2004. Spectroscopic study of extracellular polymeric substances from *Bacillus subtilis*: aqueous chemistry and adsorption effects. *Biomacromolecules* 5, 1219–1230.

Pelz, A., Wieland, K.P., Putzbach, K., Hentschel, P., Albert, K., Götz, F., 2005. Structure and biosynthesis of staphyloxanthin from *Staphylococcus aureus*. *J. Biol. Chem.* 280, 32493–32498.

Phillipson, J.D., 2001. Phytochemistry and medicinal plants. *Phytochemistry* 56, 237–243.

Sakai, K., Koyama, N., Fukuda, T., Mori, Y., Onaka, H., Tomoda, H., 2012. Search Method for inhibitors of staphyloxanthin production by methicillin-resistant *Staphylococcus aureus*. *Biol. Pharm. Bull.* 35, 48–53.

Schmitt, J., Flemming, H.C., 1998. FTIR-spectroscopy in microbial and material analysis. *Int. Biodeterior. Biodegrad.* 41, 1–11.

Schommer, N.N., Christner, M., Hentschke, M., Ruckdeschel, K., Aepfelbacher, M., Rohde, H., 2011. *Staphylococcus epidermidis* uses distinct mechanisms of biofilm formation to interfere with phagocytosis and activation of mouse macrophage-like cells 774A.1. *Infect. Immun.* 79, 2267–2276.

Sethupathy, S., Vigneshwari, L., Valliammai, A., Balamurugan, K., Pandian, S.K., 2017. L-Ascorbyl 2,6-dipalmitate inhibits biofilm formation and virulence in methicillin-resistant *Staphylococcus aureus* and prevents triacylglyceride accumulation in *Caenorhabditis elegans*. *RSC Adv.* 7, 23392–23406.

Simoes, M., 2011. Antimicrobial strategies effective against infectious bacterial biofilms. *Curr. Med. Chem.* 18, 2129–2145.

Sivasankar, C., Maruthupandian, S., Balamurugan, K., James, P.B., Krishnan, V.,

- Pandian, S.K., 2016. A combination of ellagic acid and tetracycline inhibits biofilm formation and the associated virulence of *Propionibacterium acnes* *in vitro* and *in vivo*. *Biofouling* 32, 397–410.
- Vadekeetil, A., Saini, H., Chhibber, S., Harjai, K., 2016. Exploiting the antivirulence efficacy of an ajoene-ciprofloxacin combination against *Pseudomonas aeruginosa* biofilm associated murine acute pyelonephritis. *Biofouling* 32, 371–382.
- You, J.L., Xue, X.L., Cao, L.X., Lu, X., Wang, J., Zhang, L.X., Zhou, S.N., 2007. Inhibition of *Vibrio* biofilm formation by a marine actinomycete strain A66. *Appl. Microbiol. Biotechnol.* 76, 1137–1144.
- Yuan, J.S., Reed, A., Chen, F., Stewart, C.N., 2006. Statistical analysis of real-time PCR data. *BMC Bioinf.* 7.